NJC

New Journal of Chemistry

A journal for new directions in chemistry

Accepted Manuscript

This article can be cited before page numbers have been issued, to do this please use: A. El-Kardocy , Y. A. Mostafa, N. G. Mohamed, M. N. Abo-Zeid, N. A. Hassan, H. F. Hetta and A. M. Abdel-Aal, *New J. Chem.*, 2020, DOI: 10.1039/D0NJ01194K.

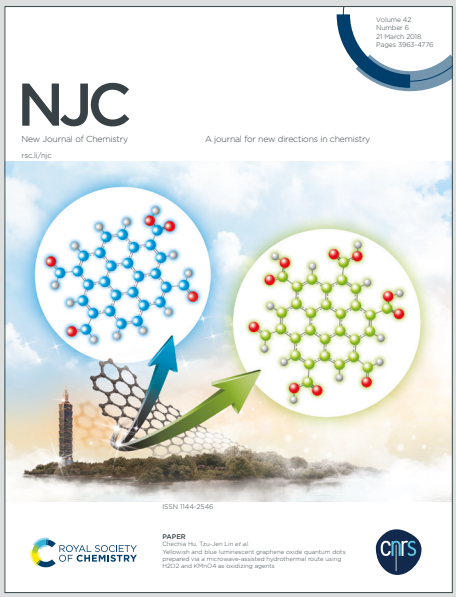

View Article Online
DOI: 10.1039/D0NJ01194K

ARTICLE

CK2 inhibition, lipophilicity and anticancer activity of new N^1 versus N^2-substituted tetrabromobenzotriazole regioisomers

Received 00th January 20xx,
Accepted 00th January 20xx

DOI: 10.1039/x0xx00000x

Ahmed El-Kardocy [1], Yaser A. Mostafa [2], Noha G. Mohamed [1], Mohammad Nabil Abo-Zeid [3], Nivin A. Hassan [4], Helal F. Hetta [5,6], Abu-Baker M. Abdel-Aal [1,2,*]

Abstract: A new series of antiproliferative Casein Kinase 2α (CK2α) inhibitors were synthesized incorporating either a hydrophilic group (carboxylic or hydrazide) or a hydrophobic group (ester) at N^1 or N^2 of 4,5,6,7-tetrabromobenzotriazole (TBBt). New compounds were prepared via *N*-alkylation of TBBt followed by base-catalysed hydrolysis or hydrazinolysis. All compounds demonstrated low sub-micromolar inhibition of CK2α and antiproliferative activity against both breast and lung cancer cell lines (MCF-7, A549, respectively) at low micromolar concentrations with N^2-regioisomers exhibiting higher activity than their corresponding N^1-isomers. The most active compound incorporates acetic acid hydrazide moiety at the N^2 of TBBt triazole nucleus with IC_{50} at 0.131 µM (CK2α), 9.1 µM (MCF-7) and 6.3 µM (A549). It induced apoptosis in MCF-7 cell line through upregulation of bax (pro-apoptotic gene) four to five times higher than the corresponding ester or acid analogues. Molecular docking suggests the hydrophilic group at N^2 of the TBBt triazole nucleus provides binding with important residues (Asp175, Lys68 and Trp176) in the ATP binding site of the CK2α enzyme. We are the first to experimentally estimate lipophilicity of TBBt derivatives. Our study demonstrated that TBBt hydrazides are more lipophilic than their corresponding acids in contrast to the contradicting calculated lipophilicity using four well-known software programs. This may explain the higher anticancer activity of the most active hydrazide over its corresponding acid despite their nearly equipotent enzyme inhibition.

Keywords: Kinase CK2; anticancer; apoptosis; lipophilicity; benzotriazole

Introduction

Oncogenic transformations are associated with activation and overexpression of several protein kinases involved in the regulation of critical cellular processes such as growth, differentiation, signalling and transduction[1, 2]. Protein kinases activate other proteins by transferring a phosphate group from adenosine triphosphate (ATP) to serine, threonine or tyrosine in these proteins [3]. Inhibition of protein kinases is becoming the most attractive therapeutic strategy with over 20 kinase targeting drugs have been approved as anticancer agents over the past decade and hundreds are currently in clinical trials for various diseases[4-6]. For instance, casein kinase 2 (CK2) is a serine/threonine protein kinase overexpressed in many cancers including acute myeloid leukaemia, breast, prostate and lung cancer[7, 8]. In the last decade, a great number of CK2 inhibitors have been developed including polyhalogenated benzimidazoles, polyhalogenated benzotriazoles, indolo and pyrroloquinolines with the most successful example, silmitasertib (CX-4945, Figure 1), currently in clinical trials (ClinicalTrials.gov identifier: NCT02128282) [9-17].

4,5,6,7-tetrabromo-*1H*-benzotriazole (TBBt, Figure 1) is the most potent and selective CK2 inhibitor (Ki = 0.4 µM) among polyhalogenated benzotriazoles and second after DMAT in the polyhalogenated benzimidazoles[18-21]. The catalytic center of CK2α is relatively smaller than the active sites of other kinases[22]. The presence of four bromine atoms is optimal for binding of the molecule to a hydrophobic pocket in the ATP-binding site of the enzyme forming halogen bonds and hydrophobic interactions with essential hydrophobic amino acid residues[23,

[a, 1] *Student research unit, Faculty of Pharmacy, Assiut University, Assiut 71526, Egypt.*
[b, 2] *Department of Pharmaceutical Organic Chemistry, Faculty of Pharmacy, Assiut University, Assiut 71526, Egypt*
[c, 3] *Department of Pharmaceutical Analytical Chemistry, Faculty of Pharmacy, Assiut University, Assiut 71526, Egypt*
[d, 4] *Cancer Biology Department, South Egypt Cancer Institute, Assiut University, Assiut, Egypt*
[e, 5] *Department of Medical Microbiology and Immunology, Faculty of Medicine, Assiut University, Assiut, Egypt*
[f, 6] *Department of Internal Medicine, University of Cincinnati College of Medicine, Cincinnati, OH, USA*
[g, *] *Correspondence: abubaker.elsayed@pharm.aun.edu.eg; Tel.: +02-0101-932-9596*

† Footnotes relating to the title and/or authors should appear here.
Electronic Supplementary Information (ESI) available: [details of any supplementary information available should be included here]. See DOI: 10.1039/x0xx00000x

View Article Online
DOI: 10.1039/D0NJ01194K

[24]. Despite the potency and selectivity of TBBt as CK2 inhibitor, it was found to be of low anti-proliferative potency and does not affect cell viability of cancer cell lines below 50 μM [25]. The human clinical trial candidate CX-4945 (Figure 1) which is structurally unrelated to polyhalogenated benzotriazole, occupies the same hydrophobic pocket in the ATP binding site of CK2α[13, 25, 26]. The carboxyl group of CX-4945 is strategically positioned to provide extra hydrophilic interactions between CX-4945 and CK2α (Lys68, Glu81, Asp175 and Trp176) which is not possible in the case of TBBt [13, 26, 27].

In the current study, we envisaged introduction of polar hydrophilic moieties (carboxyl acid or hydrazide) at the TBBt triazole ring (Figure 1) may provide novel derivatives capable of forming strong polar interactions with the area outside the hydrophobic pocket of the CK2 ATP binding site compared to their hydrophobic ester analogues. Introduction of the polar groups at *N*[1] or *N*[2] of the triazole nucleus would give information about the importance of their orientation in the ATP binding site for CK2 inhibitory activity. Hydrophilic groups will alter important physicochemical properties of the polyhalogenated benzotriazole scaffold such as lipophilicity which affect their cell membrane penetration and anti-proliferative activity. To the best of our knowledge, there are no reports for experimentally estimated lipophilicity of polyhalogenated benzotriazole derivatives.

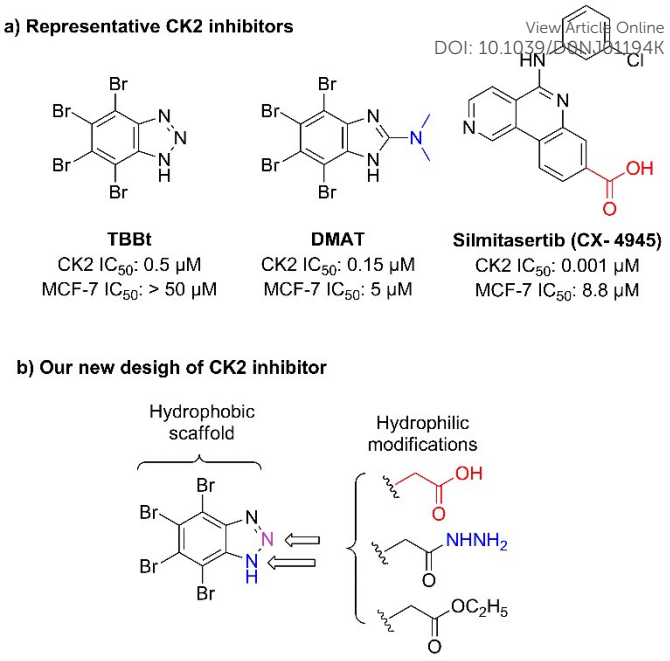

Figure 1: Design of new anti-proliferative CK2 inhibitors. The polar ester, hydrazide or acid functional groups are introduced at either N1 or N2 of the TBBt scaffold.

Scheme 1: Synthesis
ClCH$_2$COOCH$_2$CH$_3$, K$_2$C
HNO$_3$, reflux, 48h; b)
anol, reflux, 1h.

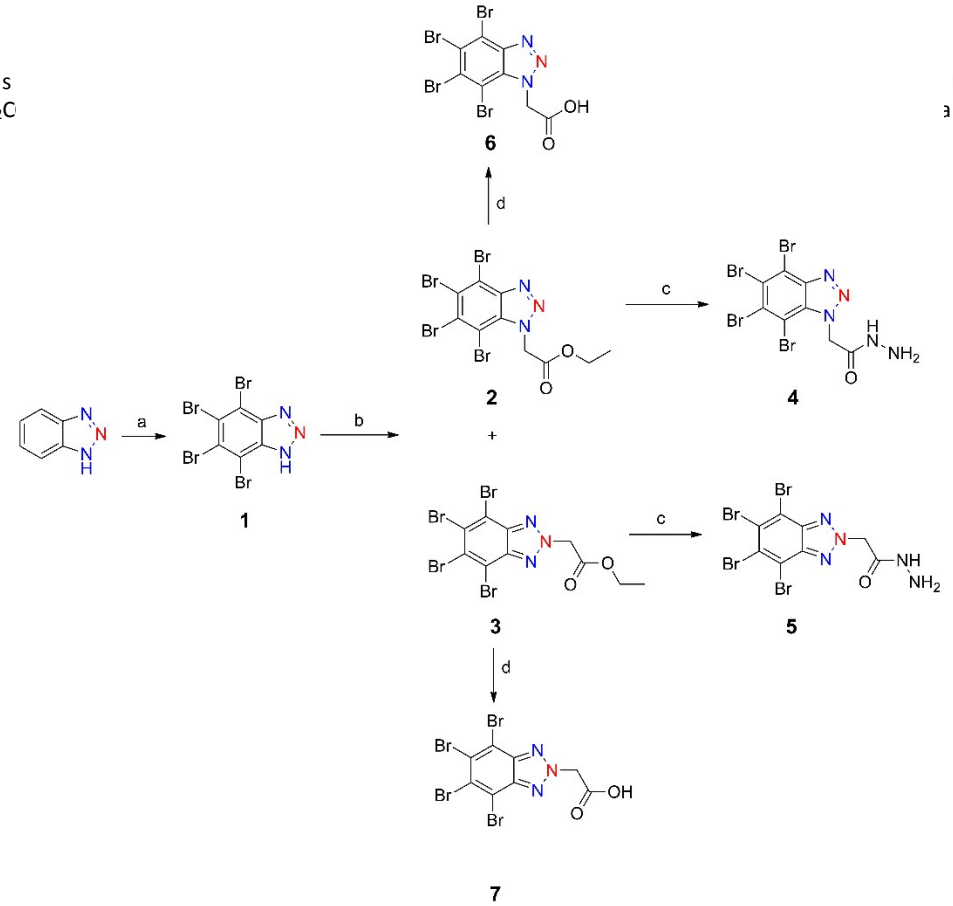

View Article Online
DOI: 10.1039/D0NJ01194K

In the current study, we report the lipophilicity of TBBt and our new *N*[1] and *N*[2]-substituted TBBt regioisomers as estimated theoretically and experimentally to find correlations between lipophilicity and anticancer activity. The aim was to modify the polyhalogenated benzotriazole scaffold with a minimal polar functional group to improve CK2 inhibitory activity and to obtain polyhalogenated TBBt derivatives capable of inhibiting cancer cell proliferation at low concentrations.

2. Results and discussion

2.1. Chemistry

4,5,6,7-tetrabromobenzotriazole (**1**) was synthesized via extensive bromination of benzotriazole in refluxing concentrated nitric acid as previously reported[28]. New target compounds **2-7** were efficiently synthesized via *N*-alkylation followed by hydrazinolysis or base catalyzed hydrolysis, Scheme 1. N-alkylation was achieved by refluxing **1** with ethyl chloroacetate in acetone, potassium carbonate and tetrabutyl ammonium bromide as phase transfer catalyst. A mixture of N^1 and N^2-acetate regioisomers (**2** and **3**) was obtained in a ratio of 3:2 in a good total yield. Separation of these two regioisomers was successfully performed using silica gel column chromatography and gradient elution of hexane: ethyl acetate (12:1 to 7:1). N-alkylation was confirmed by the appearance of ester carbonyl group and aliphatic C-H stretching vibrations in the IR spectrum of **2** (1734.6 and 2925.2 cm^{-1}) and **3** (1743.2, 2967.9 cm^{-1}). Additionally, the *N*-methylene protons appears as singlet peak at 5.89 and 5.94 ppm in the H^1-NMR spectrum of **2** and **3**, respectively**.** While, the two isomers exhibit quite similar IR and H^1-NMR spectra, their C^{13}-NMR spectra (Figure 2) are fundamentally distinguishable. For instance, the N^1-acetate isomer (**2**) has six peaks in the aromatic region (100-150 ppm) corresponding to the benzotriazole ring carbons. In contrast, the N^2-acetate isomer (**3**) has only three peaks in the same region due to the existence of a plane of molecular symmetry.

Having the two esters in hand, we were able to obtain the corresponding hydrazides and acids. Hydrazinolysis was achieved by refluxing each ester (**2-3**) in excess hydrazine hydrate and ethanol for 6 h. Pure hydrazide derivatives (**4**-**5**) simply crystallized out when the reaction was left to cool overnight and obtained in a satisfactory yield by simple filtration and washing with ethanol. Hydrazides were identified by the appearance of NH and carbonyl vibrations in the IR spectra of **4** (3316 and 1663 cm^{-1}) and **5** (3304 and 1661 cm^{-1}). Moreover, the ethyl protons of the starting esters disappear in the H^1-NMR spectra of the product hydrazides. Instead, additional peaks appear at 4.4 ppm and 9.5 ppm corresponding to the NH_2 and NH protons with upfield shifting of the *N*-methylene protons to 5.51 ppm. The acid derivatives (**6**-**7**) were obtained by base-catalyzed hydrolysis of the corresponding esters (**2**-**3**) using 5% KOH. The products were obtained pure after acidification of the reaction mixture and were confirmed by the appearance of broad OH stretching vibration at 3200-2500 cm^{-1} and acid

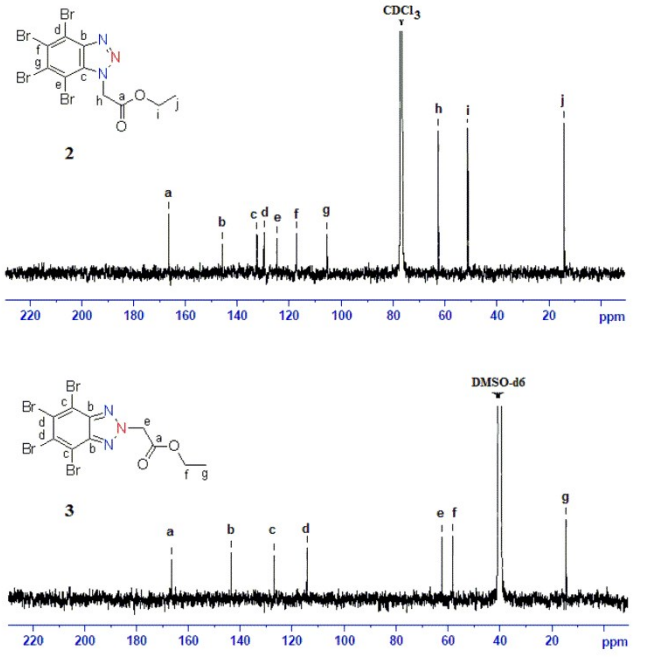

Figure 2: C^{13}-NMR spectra demonstrate distinct pattern for purified regioisomers 2 and 3.

carbonyl stretching vibration at 1736 and 1732 cm^{-1} in the IR spectrum of **6** and **7**, respectively. The H^1-NMR spectra of both compounds show only one singlet peak for the *N*-methylene at 5.7-5.8 ppm. The purity of all compounds was confirmed using elemental analysis and were found to exceed 99.6%.

2.2. CK2 enzyme inhibition and molecular modelling study

All tested compounds have the TBBt scaffold and differ only in the position and nature of substituent at the triazole N^1 or N^2. Except for compound **2**, other tested compounds showed CK2 inhibitory activity at sub-micromolar concentrations (Figure 3a). The most potent derivatives (**5** and **7**) were five times more potent than the parent TBBt (**1**) with their CK2 IC50 at 0.131 and 0.098 µM, respectively. Both compounds have their hydrophilic groups (hydrazide and carboxyl) substituted at N^2 of the triazole nucleus. Their respective regioisomers (**4** and **6**) were four to five times less potent which indicates the importance of the position of hydrophilic group for CK2 enzyme inhibitory activity. Similarly, ester derivatives (**2** and **3**) were three to four times less potent than their corresponding acid derivatives (**6** and **7**).

Molecular modelling study was done to explain the differences in CK2 enzymatic inhibitory activity of tested compounds in comparison to CX-4549. For instance, CX-4549 binds to key amino acids in the ATP binding site of CK2α including direct binding to Val116 and Lys68 and indirect binding via two conserved water molecules to Asp175, Glu81 and Trp176 [26]. Docking of compounds **2-7** showed that these compounds occupy the same hydrophobic pocket in the CK2 ATP binding site like their parent compound (**1**) and CX-4945 (Figure 3b-c,

View Article Online
DOI: 10.1039/D0NJ01194K

Supporting information S2). The most potent CK2 enzyme inhibitors of the tested compounds (**5** and **7)** establish the essential direct interactions with Val116, Lys68 and Asp175 and indirect interactions with Glu81 and Trp176 through two

(a) (b)

Figure 3: a) CK2 IC_{50} values of tested compounds (**1-7**) represented as means ±sd of three independent experiments statistically analyzed using t-test, **; p <0.0, *; p <0.05, ns; p >0.05), b) Superposition of CX-4945 and compound (**5**) at ATP binding site of human CK2 enzyme PDB code 3PE1, c) 2D representation of **(2), (5)** and **(7)** docked at ATP binding site of CK2α, d) Dose dependent CK2α inhibition of tested compounds **(2, 5** and **7)** at concentration range 0.0001-5 µM represented as mean ± sd of three independent experiments

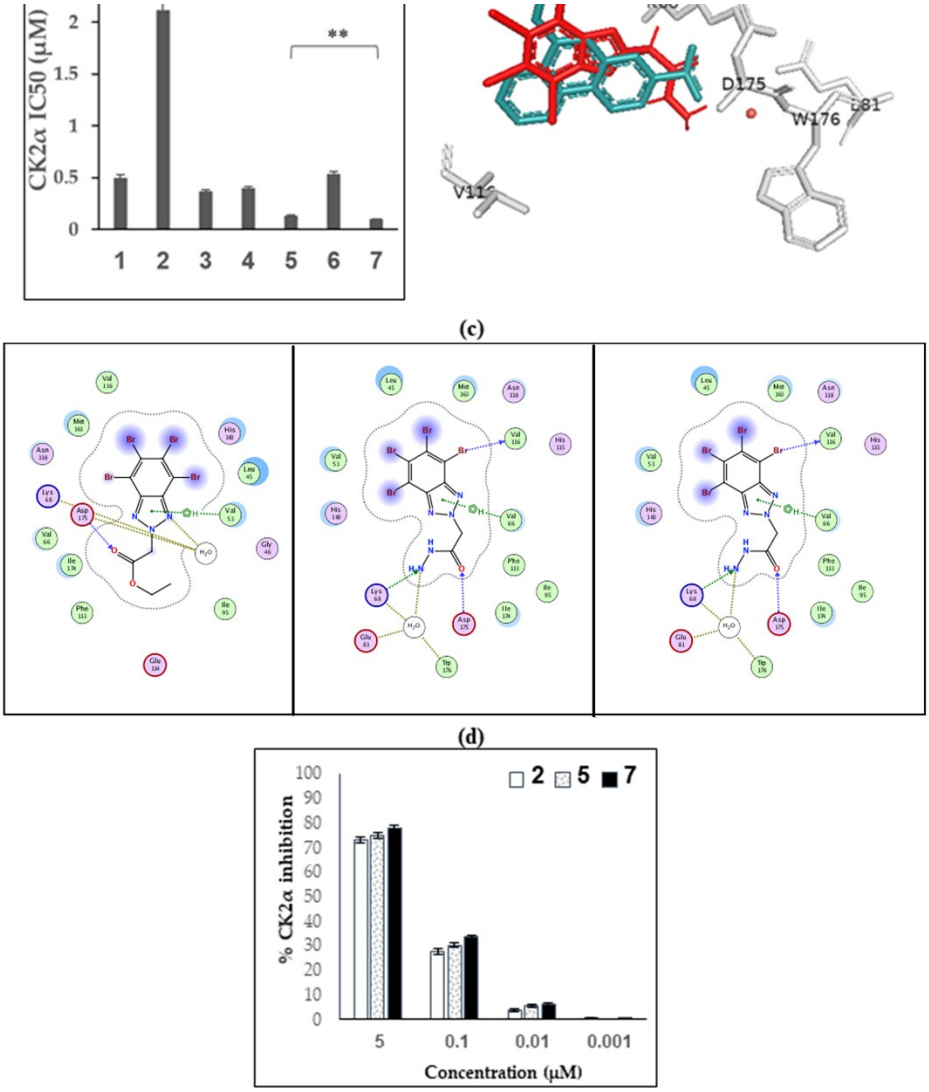

water molecules. The triazole ring assesses hydrophobic interaction with Val66 (**5**) or Ile 174 (**7**). Moreover, the hydrazide group of **5** and carboxyl group of **7** are super-positioned as the carboxyl group of CX-4945 (Figure 3b). Both compounds have their hydrophilic groups (hydrazide and carboxyl, respectively) substituted at N^2 of the triazole nucleus. The marked decrease in CK2 enzyme inhibition by compounds **4** and **6** compared to their corresponding isomers (**5** and **7**) may be explained by the loss of direct binding of **4** to Asp175 and water mediated binding of **6** to Trp176 and Glu81 due to changing the position of hydrophilic groups (carboxyl and hydrazide) from N^2 to N^1 of the triazole nucleus. Similarly, esterification of the carboxylic acid group in compound **2** and **3** leads to loss of the direct essential inhibitory hydrogen bonding to Val 116 and water bridged bonding to Glu81 and Trp176. In the N^2 regioisomers there was no difference in the mode of binding of hydrazide group in **5** and carboxyl group in **7**. However, there was a variation between them in the N^1 isomers. As shown in supporting information S1c, hydrazide group in **4** couldn't establish the direct bond to Asp125 while carboxyl group in **6** doesn't establish the indirect interaction with Glu81 and Trp176 via water molecule. This may explain the converging IC_{50} of **5** and **7** (0.098 µM and 0.13 µM respectively) and the variable IC_{50} in **4** and **6** (0.39 µM and 0.54 µM respectively). The docking results are consistent with the concentration dependent CK2α inhibition of tested compounds

View Article Online
DOI: 10.1039/D0NJ01194K

and their order of inhibitory activity (**2 < 5 < 7**) as shown in Figure 3d. Both CK2α inhibition assay and docking studies illustrated clearly that the nature and position of substituting group of tested compounds are critical factors for the interaction of tested compounds with the CK2 enzyme.

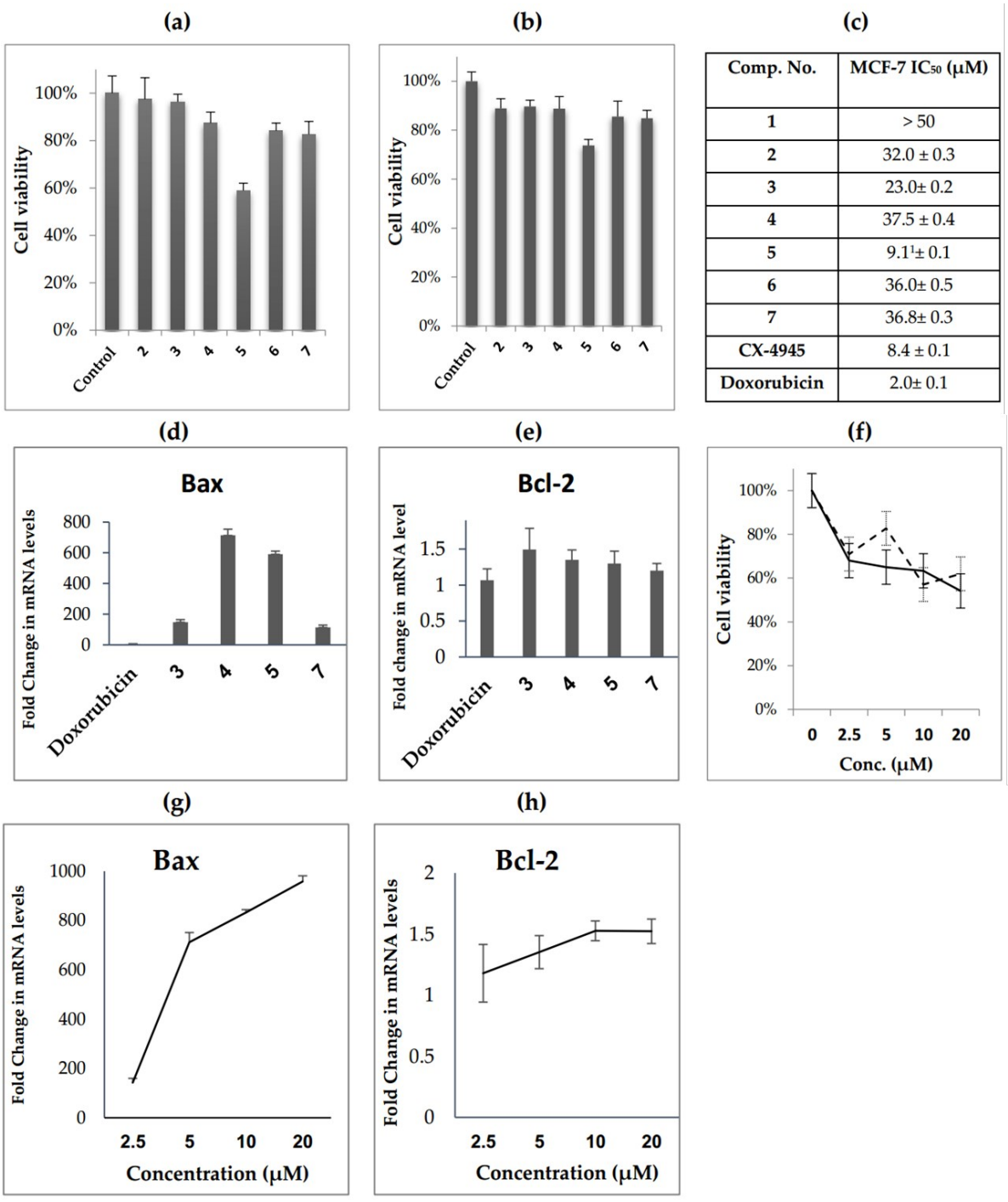

Comp. No.	MCF-7 IC_{50} (μM)
1	> 50
2	32.0 ± 0.3
3	23.0± 0.2
4	37.5 ± 0.4
5	9.1[1]± 0.1
6	36.0± 0.5
7	36.8± 0.3
CX-4945	8.4 ± 0.1
Doxorubicin	2.0± 0.1

Figure 4: Antiproliferative activities of tested compounds: a) cell viability of human lung cancer cell line (A549) treated with tested compounds at 5 μM for 48 h.; (b) cell viability of human breast cancer cell line (MCF-7) treated with tested compounds at 5 μM for 48 h.; c) IC_{50} (MCF-7) of tested compounds, [1]IC_{50} (A549) of **5** is 6.31μM; d) Fold change in expression levels of BAX mRNA following treatment of MCF-7 cells with tested compounds at 10 μM for 48 h; e) Fold change in expression levels of BCL2 mRNA following treatment of MCF-7 cells with tested compounds at 10 μM for 48 h; f) Effect of compound **5** concentration on cell viability of cancer cell lines represented by solid line (A549) and dashed line (MCF-7); g) Effect of compound **4** concentration on BAX mRNA expression; h) Effect of compound **4** concentration on BCL2 mRNA expression.

View Article Online DOI: 10.1039/D0NJ01404K

2.3. In-vitro Anti-proliferative activity

The anti-proliferative assay was performed against human breast and lung adenocarcinoma cell lines (MCF-7 and A549; respectively) using 3-(4,5-dimethylthiazol-2-yl)-2,5-diphenyltetrazolium bromide (MTT) colorimetric assay as described by T. Mosmann[29]. Cell viability of cancer cell lines were evaluated after 48 h treatment with tested compounds, Figure 4. Tested compounds exhibited comparable pattern of anti-proliferative activity in both cell lines at 5 μM concentration where hydrazides (**4** and **5**) were more effective than their corresponding esters (**2** and **3**). A549 cells were slightly more sensitive to the tested compounds than MCF-7 cells which lack caspase 3 and have impaired apoptosis. Compound **5** demonstrated significantly higher anti-proliferative effect than its corresponding regioisomer **4**.

All compounds were tested on MCF-7 at several concentration in the range of 2.5-20 μM to determine their IC_{50} (Figure 4c, f and supporting information S2). IC_{50} is the concentration of a tested compound which decreases the percentage of viable cells to a half in comparison to negative control cells treated with only media and positive control cells treated with doxorubicin as a reference anticancer drug. Compounds **2, 4, 6** and **7** demonstrated moderate anti-proliferative activity with IC_{50} for MCF-7 cell line in the range of 32-37.5 μM which is markedly better than the parent **1**. Compound **3** which has the ester functional group at N^2 of the triazole ring was more potent with IC_{50} = 23 μM. Compound **5** which has the hydrazide functional group at N^2 of the triazole ring exhibited the highest potency in MCF-7 and A549 cell lines (IC_{50} = 9.1, 6.3 μM, respectively, Figure 4c) and was equipotent to CX-4945, the most successful CK2 inhibitor in clinical trials. It exhibited a concentration dependent antiproliferative activity in both cancer cell lines at concentration range (0-20 μM) as shown in Figure 4f.

2.4. Quantitative real-time PCR evaluation of apoptotic genes expression levels.

Bax and Bcl-2 are two genes playing opposing roles in the regulation of cellular apoptosis. Their expression leads to two different proteins: bax (pro-apoptotic) and bcl-2 (anti-apoptotic) . In this study, the levels of mRNA expression of Bax and Bcl-2 genes in MCF-7 cells, treated with tested compounds at 10 μM, was determined using quantitative real-time PCR (qRT-PCR) technique. Interestingly, all treated cells (Figure 4d-e) exhibited increase of the Bax mRNA expression levels (upregulation) and non-significant change of Bcl-2 m-RNA expression levels. Both hydrazide derivatives (**4-5)** showed four to five times higher levels of Bax m-RNA than the corresponding ester (**3**) or acid (**7**). The most potent compound (**4**) demonstrated a concentration-dependent up-regulation of Bax m-RNA (Figure 4g) with non-significant change in Bcl-2 m-RNA expression levels (Figure 4h) at the tested concentration range (0-20μM).

A comparison of results from the CK2 enzyme inhibition Figure 3a) and anti-proliferative activity (Figure 4c), gave different order of activity for tested compounds. For instance, both the hydrazide (**5**) and the acid (**7**) achieved similar levels of CK2 enzyme inhibition which is three times more potent than their corresponding ester **3.** The hydrazide **5** was significantly more cytotoxic and apoptotic than both **3** and **7** (Figure 4d-e). The unparallel between CK2 enzyme inhibitory and cytotoxic activities is not fully explained. In order to find a possible explanation of these differences, we decided to estimate the lipophilicity of the tested compounds both theoretically and experimentally as lipophilicity may affect cell penetration properties and hence explain the difference between enzyme and cell-based activities.

2.5. Lipophilicity study

Lipophilicity is a physicochemical property that influences pharmacokinetics, pharmacodynamics and toxicity of drugs as a result of its impact on their passive diffusion through biological membranes. According to IUPAC, lipophilicity is the affinity of a compound for a lipophilic environment. It is generally assessed by the distribution behavior of the drug in biphasic systems such as liquid-liquid systems (e.g. 1-octano/water) or solid-liquid systems (e.g. RP-HPLC or RP-TLC)[30]. A common parameter used for expression of the lipophilicity of a drug molecule, is the partition coefficient, P, that represents partitioning of a drug between an aqueous and a non-aqueous phase. 1-octanol/water solvent system has been recognized as the reference system using the shake-flask technique for determination of the partition coefficient, $P_{O/W}$, of drug. Lipophilicity is usually expressed as log $P_{O/W}$ which is defined as the logarithm of the ratio of concentration of a neutral, non-ionized substance, in 1-octanol to that in water[31].

Due to practical difficulties of the shake-flask method, reversed-phase (RP) chromatography is frequently used for the estimation of lipophilicity of drugs, mainly RP-HPLC and RP-TLC, relying on their retention factors via simulating 1-octanol–water system. RP-TLC offers many advantages over other methods as it is cost effective, rapid and high throughput technique, consumes small volume of solvents and requires simple equipment and hence it is widely used for experimental estimation of lipophilicity[32].

Computation methods using different computer programs can be used to generate calculated Log P values for the studied compounds based on atom contributions, fragment contributions, atom/fragment contributions or atom-type electrotopological-state indices and neural network modeling for instance, MOE, Molsoft, ChemDraw and ALOGPS.

2.5.1. Theoretical lipophilicity calculation of N^1 and N^2-substituted TBBt derivatives

Lipophilicity of tested compounds were theoretically calculated using four different software programs (Molsoft, MOE, ChemDraw and ALOGPS 2.1). Calculated LogP (o/w) values of tested compounds (**1-7, Table 1**) were in the range of 1.92–5.04. The order of lipophilicity of tested compounds were different amongst different software programs. The highest lipophilic compound is the ester derivative (**3**) as calculated by Molsoft, ChemDraw and ALOGPS 2.1 software programs. MOE software predicts the parent compound (**1**) to be the highest lipophilic in the series. The highest hydrophilic compound as calculated by all software is the hydrazide derivative (**4**) with Calcd. LogP

View Article Online
DOI: 10.1039/D0NJ01104K

(o/w) in the range 1.92-3.20 which is about one digit less than the calculated values of the acid derivatives (**6** and **7**).

In conclusion, lipophilicity prediction software programs give contradicting results despite the structural similarity among the tested compounds and are not reliable to comprehend on the difference in antiproliferative activity of tested compounds. Previous studies on polyhalogenated benzotriazoles and benzimidazoles were relying on calculated lipophilicity which may have complicated interpretation of their anticancer activity [33, 34]. However up to our knowledge there was no attempts to experimentally measure lipophilicity of any polybrominated benzimidazole or benzotriazole derivatives. We thought experimental estimation of TBBt derivatives lipophilicity would give unprecedent information and may provide clues about lipophilicity-antiproliferative activity relationship.

Table 1: Calculated log P values using different software programs

Comp. No.	Calcd. LogP (o/w)			
	MOE	Molsoft	ChemDraw	ALOGPS 2.1
1	4.67	3.91	4.26	3.94
2	4.16	4.05	4.07	4.28
3	4.31	4.44	5.04	4.38
4	2.41	1.92	2.71	3.20
5	2.56	2.31	3.04	3.55
6	3.55	3.22	3.84	3.41
7	3.70	3.62	4.15	3.76

2.5.2. Experimental lipophilicity estimation of N^1 and N^2-substituted TBBt derivatives using RP-TLC

Lipophilicity parameters were experimentally measured using RP-TLC method as described elsewhere [31]. Three mobile phases were used consisting of different proportions of water and organic modifiers (acetonitrile, acetone and methanol). Briefly, the R_F and R_M values were obtained for each organic modifier/water system ratio (**supporting information S3-5)** and a linear regression analysis was achieved to obtain three lipophilicity chromatographic descriptors (R_{M0} , b, C_0 **Table 2**). R_{M0} is known as "the relative lipophilicity" as it describes the solute partitioning between pure water and nonpolar stationary phase. On the other hand, b (slope of the regression line) describes the specific hydrophobic surface area of the compound. In a series of structurally related compounds, b is linearly correlated with R_{M0} resulting in a linear relationship that is basic feature of the chromatographic determination of lipophilicity. C_0 represents the concentration of an organic modifier in the mobile phase for which the solute is equally distributed between the two phases, in other words, R_M = 0, R_F = 0.5. Moreover, C_0 represents the hydrophobicity per unit of specific hydrophobic surface area and It is considered more reliable in QSAR analysis as it embraces both the specific hydrophobic surface area of the solute and the chromatographically-measured lipophilicity index (R_{M0}). High values of correlation coefficients were obtained (r > 0.9831**, supporting information S3-5**) in all mobile phases, which proves the high significance of obtained descriptors for estimation of lipophilicity. The type of organic modifier (methanol, acetonitrile and acetone**, supporting information S3-5**) has small influence on relative lipophilicity (expressed as R_{M0}) or lipophilic parameter (C_0). A significant correlation exists between R_{M0} and slope (b) with r ≈ -0.9406, -0.9958 and -0.8379 in acetonitrile/water, acetone/water and methanol/water; respectively, which suggests a similar chromatographic retention mechanism for this congeneric series of studied derivatives. Moreover, a good correlation was obtained between R_{M0} and the lipophilic parameter C_0 with r ≈ 0.9250, 0.9820 and 0.8043 in acetonitrile/water, acetone/water and methanol/water; respectively.

Within the same solvent system, the difference in R_{M0} values midst tested compounds are attributed to the variation in their substituents, which affects considerably their lipophilicity. Higher R_{M0} values were found for the relatively lipophilic derivatives containing ester group (**3** and **2, Table 2**) followed by hydrazide derivatives group (**5**) which were more lipophilic than TBBt itself. N^2 derivatives were slightly more lipophilic than their corresponding N^1 derivatives. This finding is critical in understanding the differences between N^1 and N^2 regioisomers regarding their antiproliferative activity. The lowest values of R_{M0} were obtained for the more hydrophilic derivatives containing hydrazide and carboxylic acid group (**4, 7** and **6, Table 2)**. Compound **3** (containing ester group) is the highest lipophilic compound. It possesses the highest value of R_{M0}, b and C_0 in all organic modifier/water systems. According to C_0 values, compound **6** (containing carboxylic acid group) is the highest hydrophilic compound followed by its structural isomer (**7**).

Table 2: RP-TLC measured lipophilicity parameters RM0, b and C0

Comp. No.	R_{M0}			b			C_0		
	ACN	acetone	MeOH	ACN	acetone	MeOH	ACN	acetone	MeOH
1	2.02	3.16	3.59	-0.0268	-0.0428	-0.0416	75.36	73.77	86.34
2	3.42	4.15	4.01	-0.0404	-0.0512	-0.0429	84.52	81.13	93.64
3	3.64	4.51	4.69	-0.0417	-0.0543	-0.0488	87.27	83.06	96.13
4	1.39	3.07	2.26	-0.0240	-0.0412	-0.0286	57.78	74.53	79.05
5	2.56	3.69	3.88	-0.0326	-0.0470	-0.0438	78.49	78.50	88.55
6	1.45	1.51	2.62	-0.0304	-0.0271	-0.0397	47.79	55.66	65.83
7	1.28	2.11	3.38	-0.0258	-0.0351	-0.0465	49.85	60.06	72.69

Experimental results of lipophilicity were completely different in comparison with Calcd. LogP values. In contrast to Calcd. LogP (o/w), the highest lipophilic compounds as measured by RP-TLC method are the derivatives containing ester group (**3** and **2**) followed by the hydrazide derivative (**5**) while, the highest hydrophilic compounds in the series are the derivatives containing carboxylic group (**6** and **7**) followed by the hydrazide derivative (**4**).

A comparison of results from the CK2 enzyme inhibition (Figure 3a), anti-proliferative activity (Figure 4c) and experimentally estimated lipophilicity (Table 2) reveal that the hydrazide (**5**) and its acid (**7**) are nearly equipotent as CK2 inhibitors but quite different in terms of lipophilicity and antiproliferative activity. The hydrazide (**5**) is three times more potent as antiproliferative than the acid (**7**) which may be attributed to its increased lipophilicity as it would have better chance to penetrate cell membranes. There is also a significant difference between the two hydrazide regioisomers (**4** and **5**) in terms of lipophilicity, antiproliferative activity and enzyme inhibitory. While the ester **3** is more lipophilic than both **5** and **7**, it exhibited reduced cytotoxic response as a result of its reduced enzyme inhibitory activity.

4. Materials and Methods

4.1. General

All commercially available solvents and reagents were used without further purification. Melting points were measured on an electrothermal melting point apparatus [model 9100, UK], and were reported as uncorrected. Pre-coated TLC silica gel plates (kieselgel 0.25 mm, 60G F254, Merck, Germany) were used for reactions monitoring and TLC silica gel G 60 RP–18 F_{254} aluminum sheets (Merck, Germany) were used for lipophilicity estimation. TLC spots were detected using ultraviolet lamp at 254 nm wavelength (Spectroline, model CM-10, USA). Infrared spectra (KBr discs) were recorded on thermo scientific nicolet IS10 FT-IR spectrometer (thermo Fischer scientific, USA) at the Faculty of science, Assiut University, Assiut, Egypt. ^{1}H-NMR and ^{13}C-NMR spectra were scanned on AVANCE-III High Performance FT-NMR spectrometer (400 MHz Brucker) at Faculty of Science, Sohag University, Sohag, Egypt. Mass spectra were carried out on Direct Probe Controller Inlet Part TO Single Quadropole mass analyzer in Thermo Scientific GCMS model ISQ LT using Thermo X-Calibur software at the Regional Center for Mycology and Biotechnology (RCMB), Faculty of Science, Al-Azhar University, Nasr city, Cairo, Egypt. Elemental microanalyses were performed on elemental analyzer model flash 2000 thermo fisher at the Regional Center for Mycology and Biotechnology (RCMB), Faculty of Science, Al-Azhar University, Nasr city, Cairo, Egypt.

4.2. Synthesis

4.2.1. 4,5,6,7-tetrabromo-1H-benzotriazole (1)

Synthesis was performed by brominating 1H-benzotriazole according to published method[28].

4.2.2. Synthesis of N^1 and N^2 -acetate esters (2 and 3)

Ethyl chloroacetate (2.82 g, 23.0 mmol, 5 equiv.) was added to a mixture of **1** (2.00 g, 4.6 mmol, 1.0 equiv) and K_2CO_3 (1.27 g, 9.20 mmol, 2 equiv) and few crystals of tetrabutylammonium bromide as phase transfer catalyst in acetone (10 mL). The mixture was stirred at 60^{o}C for 6 h. The reaction was monitored by TLC and when completed, the solvent was evaporated to dryness. The residue was purified by column chromatography using silica gel and hexane: ethyl acetate (15:1 to 7:1) as eluent. Two regioisomers (**2** and **3**) were separated in 80% total yield.

Ethyl (4,5,6,7-tetrabromo-1H-benzo[d]triazol-1-yl)-acetate (2)

Yield: 1.15 g (48%), white crystals, m.p 140 ºC. IR (KBr, cm^{-1}): 1734.6 (CO), 2925.2 (C_2H_5). ^{1}H NMR (DMSO-d_6, 400MHz,) δ ppm: 5.89 (s, 2H, CH_2), 4.23 (q, 2H, *J* = 8.0 Hz, CH_2), 1.24 (t, 3H, *J* = 4.0 Hz, CH_3). ^{13}C NMR (DMSO-d_6, 100 MHz) δ ppm: 14.07 (CH_3), 51.31 (ester CH_2), 62.67 (N-CH_2), 105.64 (C5), 117.08 (C6), 124.73 (C4), 129.68 (C7), 132.33 (C8), 145.63 (C9), 166.35 (C=O). Anal. calcd/found. for $C_{10}H_7Br_4N_3O_2$ (520.723): C, 23.06/23.42; H, 1.35/1.59; N, 8.07/8.24.

Ethyl (4,5,6,7-tetrabromo-2H-benzo[d]triazol-2-yl)-acetate (3)

Yield: 0.766 g (32%), white crystals, m.p.182-183 ºC. IR (KBr, cm^{-1}): 1743.2 (CO), 2967.9 (C_2H_5). ^{1}H NMR (DMSO-d_6, 400MHz,) δ ppm: 5.94 (s, 2H, CH_2), 4.24 (q, 2H, *J* = 8.0 Hz, CH_2), 1.24 (t, 3H, *J* = 4.0 Hz, CH_3). ^{13}C NMR (DMSO-d_6, 100M Hz) δ ppm: 14.34 (CH_3), 58.20 (CH_2), 62.50 (N-CH_2), 117.20 (C5 &C6), 126.82 (C4 &C7), 143.37 (C8 &C9), 166.50 (C=O). Anal. calcd/found. for $C_{10}H_7Br_4N_3O_2$ (520.723): C, 23.06/23.27; H, 1.35/1.57; N, 8.07/7.92.

4.2.3. Hydrazinolysis of 2 and 3

The mixture of **2** or **3** (0.120 g, 2.3 mmol, 1.0 equiv.) and hydrazine hydrate (99 %, 0.6 g, 18.5 mmol, 8.0 equiv.) in ethanol (10 mL) was stirred and refluxed for 6 h. The mixture was left to cool for crystallization and filtered to give pure hydrazide products (**4** or **5** respectively).

2-(4,5,6,7-tetrabromo-1H-benzo[d]triazol-1-yl)acetohydrazide (4)

Yield: 0.074 g (63.5%). White crystals, mp. > 300 ºC. IR (KBr,cm^{-1}): 3316.3, 2925.1, 1663.3, 1626.6, 1545.1, 1430.2. ^{1}H NMR (DMSO-d_6, 400MHz,) δ ppm: 4.46 (br s, NH_2), 5.51 (s, CH_2), 9.47 (s, NH). 502.59 (21.03%), 504.32 (14.54%). EI-MS [*m/z* (%)]: 502.59 (M^+, 21.03%), 504.32 (M^++2,14.54%). Anal. calcd/found. for $C_8H_5Br_4N_5O$ (506.774): C, 18.96/19.24; H, 0.99/1.23; N, 13.82/14.09.

2-(4,5,6,7-tetrabromo-2H-benzo[d]triazol-2-yl)acetohydrazide (5)

Yield: 0.084 g (70.5%). White crystals, mp. > 300 ºC.. IR (KBr, cm^{-1}): 3304.2, 3053.5, 2924.0, 1661.4, 1623.6, 1545.9. ^{1}H NMR (DMSO-d_6, 400MHz,) δ ppm: 4.45 (br s, NH_2), 5.51 (s, CH_2), 9.59 (s, NH). ^{13}C NMR (DMSO-d_6, 100M Hz) δ ppm: 58.48 (CH_2),

View Article Online
DOI: 10.1039/D0NJ04104K

114.11 (C5 & C6), 126.38 (C4 & C7), 143.27 (C8 & C9), 163.94 (C=O). Anal. calcd/found. for $C_8H_5Br_4N_5O$ (506.774): C, 18.96/19.23; H, 0.99/1.07; N, 13.82/14.09.

4.2.4. Base catalyzed hydrolysis of 2 and 3

The suspension of **2** or **3** (0.075 g, mmol) in a solution of 5% NaOH (5 mL) and 2 mL ethanol was stirred and refluxed for 1 h. The mixture became clear solution. The solution was brought to pH 2-3 with conc. HCl. The white precipitate was filtered and washed with water to give pure products (**6** or **7** respectively).

2-(4,5,6,7-tetrabromo-1H-benzo[d]triazol-1-yl)acetic acid (6)

Yield 0.024 g (33.8%), white crystals mp 216 ºC. IR (KBr, cm^{-1}): 3200-2500, 3007.4, 296.4, 1736.0, 1630.3. ^{1}H NMR (DMSO-d_6,400MHz,)δ ppm: 5.77(s, 2H,CH_2). ^{13}C NMR (DMSO-d_6, 100M Hz) δ ppm: 52.1 (CH_2), 97.44, 115.95. Anal. calcd/found. for $C_8H_3Br_4N_3O_2$ (492.774): C, 19.50/19.78; H, 0.61/0.87; N, 8.53/8.78.

2-(4,5,6,7-tetrabromo-2H-benzo[d]triazol-2-yl)acetic acid (7)

Yield = 0.025 g (35.2%), white crystals mp 263. IR (KBr, cm^{-1}): 3200-2500, 2991.8, 2946.2, 1732.2, 1553.1. ^{1}H NMR (DMSO-d_6,400MHz,)δ ppm: 5.8 (s, 2H, CH_2). ^{13}C NMR (DMSO-d_6, 100M Hz) δ ppm: 58.47 (CH_2), 114.16 (C5 & C6), 126.60 (C4 & C7), 143.26 (C8 & C9), 167.86 (C=O). Anal. calcd/found. for $C_8H_3Br_4N_3O_2$ (492.774): C, 19.50/19.78; H, 0.61/0.87; N, 8.53/8.78

4.3. CK2α inhibition assay

The CK2α activity was measured using P81 filter isotopic assay as described elsewhere[35]. Briefly, a reaction solution was prepared using 20 µM substrate peptide (RRRDDDSDDD) and 10 µM ATP dissolved in 40mM HEPES buffer (50 µL, pH 7.5) with 130 mM KCl, 10 mM $MgCl_2$, and 50 µM DTT. The enzyme (hCK2α, Sigma-Aldrich) was added to the reaction mixture and was kept for 15 min at 30 ^{O}C. 10 µL of the phosphorylation reaction mixture was spotted onto the P81 filter paper followed by washing three times with 0.5 % phosphoric acid once with ethanol before scintillation counting. IC50 values for tested compounds were determined by measuring CK2α activity at concentrations ranging 0.001-5.0 µM of each compound. All tested compounds were dissolved in 0.5% DMSO.

4.4. Molecular Modelling

All molecular modeling studies were carried out on an Intel(R) Xeon(R) CPU E5-1650 3.20 GHz processor, 16 GB memory with Windows 10 Professional operating system. Molecular Operating Environment (MOE 2014.0901, Chemical Computing Group, Canada) was used as the computational software. Pymol 2.3.2 was used as viewer. The crystal structure of human Protein Kinase CK2 Catalytic Subunit co-crystallized with CX-4945 Inhibitor was downloaded from PDB (code: 3pe1). The Studied compounds were built using the builder interface of the MOE software and subjected to conformational search. Conformers were subjected to energy minimization until a RMSD gradient of 0.01 Kcal/mol and RMS distance of 0.1 Å with MMFF94X force-field and the partial charges were automatically calculated. The obtained database was then saved as MDB file to be used in the docking calculations. Docking of the energy minimized conformations was done using MOE- dock wizard. London dG was used as the scoring function (S).

4.5. MTT-based cytotoxicity assay

Cell viability was assessed using MTT assay as described elsewhere[29]. Briefly, cells were seeded into 96-well tissue culture plates in DMEM containing 10% FBS to a final volume of 200 µL/well. After 24 h of seeding, cells were treated with tested compounds, doxorubicin (positive control), or 0.5% DMSO (negative control). After 48 h incubation, media were removed and replaced with 200 µL DMEM containing 0.5 mg/mL MTT. After 2 h incubation, the supernatant was removed, and the precipitated formazan was dissolved in 200 µL DMSO and absorbance measured at 570 nm using Varioskan flash 4.00.53 microplate reader. All experiments were performed in six replicates and were calculated by subtracting blank readings. Tested compounds were screened to find the most active compound(s) capable of significantly influencing cell viability of both cell lines at low micromolar concentration (5 µM). IC_{50} was calculated as the concentration of tested compounds required to achieve 50% inhibition of cell viability
.

4.6 Evaluating the effect of tested compounds on Bax and Bcl2 genes Using Quantitative Real-Time PCR (qRT-PCR)

4.6.1- RNA extraction and reverse transcription

Total RNA was extracted, from MCF-7 cells after overnight treatment with tested compounds, using the Direct-zol™ RNA MiniPrep (Zymoresearch, Catalog No. R2053, CA, USA). The purity and concentration of RNA determined by biotech nanodrop. complementary DNA (cDNA) was synthesized using Thermo Scientific Revert Aid Reverse kit (Thermo, Waltham, MA, US).

4.6.2- Quantitative real-time PCR (qRT-PCR)

QRT-PCR was performed by 7500 fast real time PCR (Applied Biosystems, CA, USA) using QuantiTect SYBR Green PCR Kit (Qiagen, Germany) under the following conditions, hot start step at 95 °C for 7, initial denaturation for 20 sec at 95 °C, annealing and extension for 60 sec at 59 °C in 40 cycles.

Table 3: Primer sequences of the genes used for qRT-PCR experiments in this study

Genes	Forward primer	Reverse primer
Bax	5′-CCCGAGAGGTCTTTTTCCGAG-3′	5′-CCAGCCCATGATGGTTCTGAT-3′
Bcl2	5′-ATCGCTCTGTGGATGACTGAGTAC-3′	5′-ATCGCTCTGTGGATGACTGAGTAC-3′
β-Actin	5′-TGTTGTCCCTGTATGCCTCT-3′	5′-TAATGTCACGCACGATTTCC-3′

The fold change in expression of Bax and Bcl2 genes was calculated according to the $2^{-\Delta\Delta CT}$ method using β-actin as internal control gene to normalize the relative level of gene expression. The sequence of primers used in this study are listed in Table 3.

4.7. Lipophilicity estimation of tested compounds using RP-TLC chromatographic method

Chromatographic analysis was carried out on TLC silica gel G 60 RP–18 F_{254} aluminum sheets (20 × 20 cm, 0.20 mm layer thickness) that were obtained from Merck, Darmstadt, Germany. The mobile phases were prepared by mixing different proportions of double-distilled water and organic modifier. Methanol (SD Fine-Chem Limited, India), acetonitrile (Fisher Scientific U.K. Limited, United Kingdom) and acetone (Merck, Germany) were used as organic modifier for preparation of the different mobile phase systems. Standard solution (0.1 mg/mL) of each of the studied compounds was prepared in Methanol (MeOH). The content of the organic modifier; methanol, acetonitrile or acetone was varied between 50 and 95% (v/v) with an increment of 5%. The upper and lower content of organic modifier depends on the linearity between R_M and organic modifier concentration. The concentration ranges for the tested organic modifiers were used where the upper value of the range indicates that the analyte elutes near the solvent front and the lower value implies that the analyte is very near to the starting line. Then, the chromatographic chambers were saturated with the mobile phase for 0.5 h. TLC was performed on RP TLC plates (20 × 5 cm pieces). The standard solutions (5 µL) were spotted in triplicate on the plates 5 mm apart, 10 mm from the bottom edges and 5 mm from the side edges. The plates were air-dried then developed in the chromatographic chambers. Linear ascending plate development was performed until a migration distance of 35 mm from the origin was reached. After development, the plates were removed and air-dried. Then spots were localized under UV light at λ = 254 nm. Finally, the R_F values were calculated.

Rm values were derived using R_f of solutes in mobile solvent systems including water and an organic modifier such as acetone or methanol followed by construction of a relationship between Rm and C (percentage of organic modifier). A linear regression analysis was carried out using Excel 2016 (Microsoft Office) to obtain lipophilicity chromatographic descriptors (**R_{M0} , b, C_0**) as calculated from the following equations.

$$R_M = \log\left(\frac{1}{R_f} - 1\right), \qquad \mathbf{R_M = R_{M0} + bC,} \qquad C_0 = -\frac{R_{M0}}{b}$$

R_{M0} is "the relative lipophilicity" and is obtained by extrapolation of R_M value to 0% v/v of organic modifier in mobile phase system. b is the slope of the regression line. C_0 represents the hydrophobicity per unit of specific hydrophobic surface area and is the concentration of an organic modifier in the mobile phase for which the solute is equally distributed between the two phases

5. Conclusions

View Article Online
DOI: 10.1039/D0NJ01194K

The current study reports synthesis, purification and characterization of N^1 and N^2-substituted regioisomers of the most potent CK2 enzyme inhibitor; TBBt. We have shown that incorporation of hydrophilic substituents at N^2 improved TBBt CK2 enzyme inhibition and antiproliferative activities. We are first to report experimental estimation of lipophilicity for TBBt derivatives and its contradiction with their calculated values. This would shed light on the complex relationship between enzyme inhibition, lipophilicity and antiproliferative activity of TBBt derivatives. Further studies are needed to measure CK2 inhibitory activity of TBBt regioisomers in treated cells and to determine their CK2 enzyme specificity and their ability to target other kinases. This may improve our understanding of TBBt regioisomers structure-activity relationships and would impact the design of future CK2 based anticancer agents.

Supplementary Materials: The following are available online at www.xxx.com/xxx/s1, S1: Molecular modelling and docking with CK2α, S2: Cell viability of adenocarcinoma cell lines treated with 0-20 µM of compound 5 for 48 h; Table S3: The RM0 Values, C (the percentage of ACN), b (Slope) and r (Correlation Coefficient) of the Equation RM = RM0 + bC for the studied compounds ; Table S4: The RM0 Values, C (the percentage of acetone), b (Slope) and r (Correlation Coefficient) of the Equation RM = RM0 + bC for the studied compounds; Table S5: The RM0 Values, C (the percentage of MeOH), b (Slope) and r (Correlation Coefficient) of the Equation RM = RM0 + bC for the studied compounds. Figures S6: IR, H-NMR and C^{13}-NMR spectra.

Author Contributions: Conceptualization and experimental design, A. M. A.; Methodology and experimental, A. B. A., Y. A. M, M. N. A., N. A. H, N. G. M. and H. F. H; Data analysis and interpretation, A. B. A., Y. A. M, M. N. A., N. A. H., H. F. H., N. G. M; A. M. A; Manuscript writing A. B. A, N. G. M, M. N. A., A. M. A.; All authors have read and approved the final manuscript.

Conflicts of interest

There are no conflicts to declare.

Notes and references

1. M. M. Chua, C. E. Ortega, A. Sheikh, M. Lee, H. Abdul-Rassoul, K. L. Hartshorn and I. Dominguez, *Pharmaceuticals (Basel)*, 2017, **10**.
2. A. Shahraki and A. Ebrahimi, *New Journal of Chemistry*, 2019, **43**, 15983-15998.
3. I. M. Hanif, I. M. Hanif, M. A. Shazib, K. A. Ahmad and S. Pervaiz, *The international journal of biochemistry & cell biology*, 2010, **42**, 1602-1605.

View Article Online
DOI: 10.1039/D0NJ01124K

4. N. P. Shah, C. Tran, F. Y. Lee, P. Chen, D. Norris and C. L. Sawyers, *Science*, 2004, **305**, 399-401.
5. L. J. Lombardo, F. Y. Lee, P. Chen, D. Norris, J. C. Barrish, K. Behnia, S. Castaneda, L. A. Cornelius, J. Das, A. M. Doweyko, C. Fairchild, J. T. Hunt, I. Inigo, K. Johnston, A. Kamath, D. Kan, H. Klei, P. Marathe, S. Pang, R. Peterson, S. Pitt, G. L. Schieven, R. J. Schmidt, J. Tokarski, M. L. Wen, J. Wityak and R. M. Borzilleri, *J Med Chem*, 2004, **47**, 6658-6661.
6. K. S. Bhullar, N. O. Lagarón, E. M. McGowan, I. Parmar, A. Jha, B. P. Hubbard and H. P. V. Rupasinghe, *Mol Cancer*, 2018, **17**, 48-48.
7. D. W. Litchfield, *Biochem J*, 2003, **369**, 1-15.
8. M. Saravanabhavan, V. N. Badavath, S. Maji, S. Muhammad and M. Sekar, *New Journal of Chemistry*, 2019, **43**, 17231-17240.
9. R. F. Marschke, M. J. Borad, R. W. McFarland, R. H. Alvarez, J. K. Lim, C. S. Padgett, D. D. V. Hoff, S. E. O'Brien and D. W. Northfelt, *Journal of Clinical Oncology*, 2011, **29**, 3087-3087.
10. I. Kufareva, B. Bestgen, P. Brear, R. Prudent, B. Laudet, V. Moucadel, M. Ettaoussi, C. F. Sautel, I. Krimm, M. Engel, O. Filhol, M. L. Borgne, T. Lomberget, C. Cochet and R. Abagyan, *Scientific Reports*, 2019, **9**, 15893.
11. G. Cozza, *Pharmaceuticals (Basel)*, 2017, **10**, 1-23.
12. B. Bestgen, Z. Belaid-Choucair, T. Lomberget,M. Le Borgne, O. Filhol and C. Cochet, *Pharmaceuticals (Basel)*, 2017, **10**.
13. A. Siddiqui-Jain, D. Drygin, N. Streiner, P. Chua, F. Pierre, S. E. O'Brien, J. Bliesath, M. Omori, N. Huser, C. Ho, C. Proffitt, M. K. Schwaebe, D. M. Ryckman, W. G. Rice and K. Anderes, *Cancer research*, 2010, **70**, 10288-10298.
14. J. Zhang, P. L. Yang and N. S. Gray, *Nature Reviews Cancer*, 2009, **9**, 28-39.
15. P. Cohen, *Nat Rev Drug Discov*, 2002, **1**, 309-315.
16. J. Dancey and E. A. Sausville, *Nature Reviews Drug Discovery*, 2003, **2**, 296-313.
17. A. K. Jain, C. Karthikeyan, K. D. McIntosh, A. K. Tiwari, P. Trivedi and A. DuttKonar, *New Journal of Chemistry*, 2019, **43**, 1202-1215.
18. M. A. Pagano, F. Meggio, M. Ruzzene, M. Andrzejewska, Z. Kazimierczuk and L. A. Pinna, *Biochem Biophys Res Commun*, 2004, **321**, 1040-1044.
19. P. Zień, M. Bretner, K. Zastąpiło, R. Szyszka and D. Shugar, *Biochemical and Biophysical Research Communications*, 2003, **306**, 129-133.
20. M. A. Pagano, M. Andrzejewska, M. Ruzzene, S. Sarno, L. Cesaro, J. Bain, M. Elliott, F. Meggio, Z. Kazimierczuk and L. A. Pinna, *J Med Chem*, 2004, **47**, 6239-6247.
21. P. Zien, J. S. Duncan, J. Skierski, M. Bretner, D. W. Litchfield and D. Shugar, *Biochim Biophys Acta*, 2005, **1754**, 271-280.
22. H. R. Stefania Sarnoa;1, Flavio Meggioa, Maria Ruzzenea, Stephen P. Daviesb, and D. S. Arianna Donella-Deanaa, Lorenzo A. Pinnaa;*, *FEBS Letters*, 2001.
23. R. BATTISTUTTA, E. D. MOLINER, S. SARNO, G. ZANOTTI and L. A. PINNA, *Protein Science*, 2001, **10**, 2200–2206.
24. R. Wąsik, M. Łebska, K. Felczak, J. Poznański and D. Shugar, *The Journal of Physical Chemistry B*, 2010, **114**, 10601-10611.
25. P. Borowiecki, A. M. Wawro, P. Winska, M. Wielechowska and M. Bretner, *Eur. J. Med. Chem.*, 2014, **84**, 364-374.
26. A. D. Ferguson, P. R. Sheth, A. D. Basso, S. Paliwal, K. Gray, T. O. Fischmann and H. V. Le, *FEBS Lett*, 2011, **585**, 104-110.
27. R. Battistutta, G. Cozza, F. Pierre, E. Papinutto, G. Lolli, S. Sarno, S. E. O'Brien, A. Siddiqui-Jain, M. Haddach, K. Anderes, D. M. Ryckman, F. Meggio and L. A. Pinna, *Biochemistry*, 2011, **50**, 8478-8488.
28. R. Szyszka, N. Grankowski, K. Felczak and D. Shugar, *Biochemical and Biophysical Research Communications*, 1995, **208**, 418-424.
29. T. Mosmann, *Journal of immunological methods*, 1983, **65**, 55-63.
30. Ł. Komsta, M. Waksmundzka-Hajnos and J. Sherma, *Thin Layer Chromatography in Drug Analysis*, 2014.
31. S. Šegan, D. Opsenica and D. Milojković-Opsenica, *Journal of Liquid Chromatography & Related Technologies*, 2019, **42**, 238-248.
32. R. Mannhold, K. Dross, C. Sonntag, V. Pliška, B. Testa and H. van de Waterbeemd, *Lipophilicity in Drug Action and Toxicology*, 1996.
33. E. Łukowska-Chojnacka, P. Wińska, M. Wielechowska, M. Poprzeczko and M. Bretner, *Bioorganic & Medicinal Chemistry*, 2016, **24**, 735-741.

View Article Online
DOI: 10.1039/D0NJ01194K

34. K. Chojnacki, P. Wińska, K. Skierka, M. Wielechowska and M. Bretner, *Bioorganic Chemistry*, 2017, **72**, 1-10.
35. B. B. Olsen, T. Rasmussen, K. Niefind and O. G. Issinger, *Molecular and cellular biochemistry*, 2008, **316**, 37-47.

View Article Online
DOI: 10.1039/D0NJ01194K

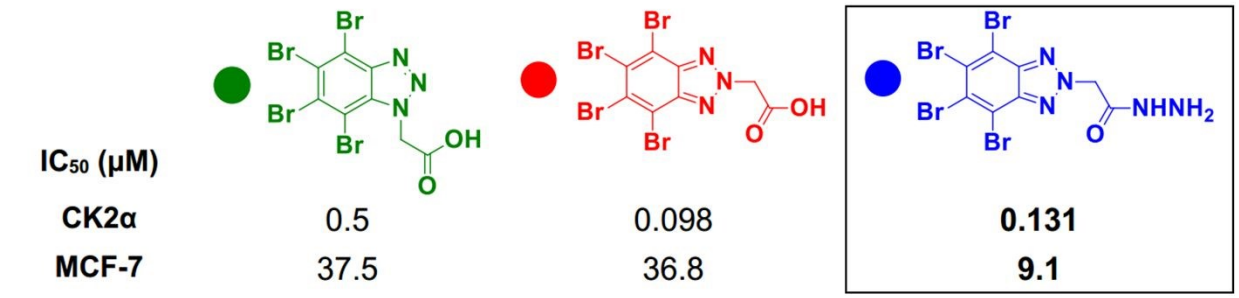

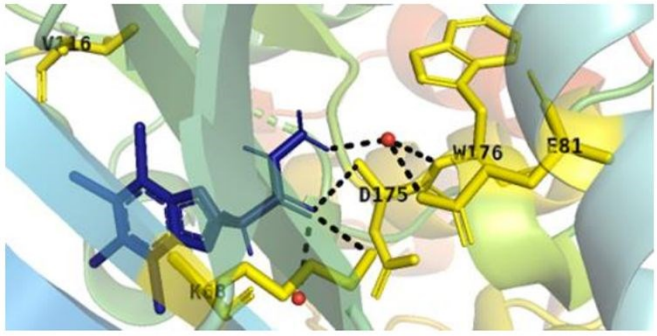

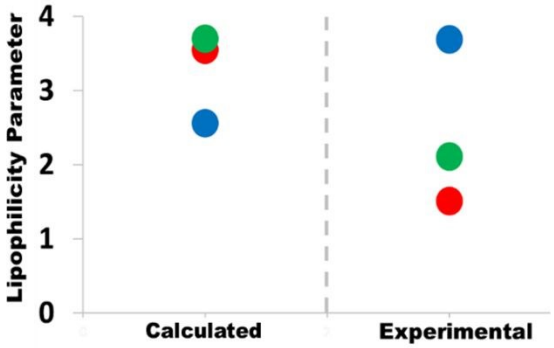

Both type and position of polar group substitution in polybrominated benzotriazoles dramatically change their lipophilicity, kinase inhibition and anticancer activity.